ISSN 2989-0705 (Online)|Vol 2|Issue 1|January 2024

Journal of Applied Learning | BMS CAMPUS make learning happen

Ecologically friendly synthesis of silver nanoparticles by a variation of *Dianthus caryophyllus* leaves. Analyzing their antioxidant, antibacterial, photocatalytic activities, melamine adulteration, and cytotoxicity.

Eleena Maria Rosamystica Mahendran[1] and Mathivathani Kandiah[1*]

[1]School of Management, Business Management School (BMS), Sri Lanka

[*]mathi@bms.ac.lk

Abstract

Among the various nanoparticles that have been employed for the use in biomedical applications, silver nanoparticles (AgNP's) are one of the most significant and intriguing nanomaterials. Therefore, this study was conducted to examine their characteristics. A variety of Dianthus caryophyllus were used to make water extracts (WE) and by combining the WE and silver nitrate ($AgNO_3$), nanoparticles were synthesized. Characterization of these AgNP's were accomplished using UV-spectrophotometry and scanning electron microscopy (SEM). SEM analysis shows that the AgNP is cuboidal in shape and around 50nm in size. These WEs had their phytochemical characteristics examined, and on both the WE and AgNP's, total flavonoid content (TFC), total phenolic content (TPC), total antioxidant capacity (TAC), and 2,2-diphenyl-1-picrylhydrazylhydrate (DPPH) assays were performed. Methyl red (MR) was used to test the pink-AgNP's photocatalytic activity, and pink-AgNP was also used to identify melamine in milk. All five AgNP's and five WEs underwent antibacterial testing using *Escherichia coli* (*E. coli*) *and Staphylococcus aureus* (*S. aureus*) and with the use of brine shrimps, the pink AgNP's cytotoxicity was evaluated. The results of these tests confirmed that higher TFC and DPPH activity was seen in WE's and that higher TPC and TAC activity was seen in AgNP's. The use of sodium borohydride ($NaBH_4$) under sunlight exhibited increased degradation activity of the dye molecule. The detection of melamine using pink-AgNP was seen in 1000ppm, 100ppm, 10ppm, 1ppm and 0.1ppm of melamine, while when another method for detection using, WE and $AgNO_3$ was done, melamine was not detected in 1000ppm, the cytotoxic evaluation revealed 100% viability of the shrimps 24hrs after pink-AgNP addition. This study was useful in identifying different properties of AgNP's synthesized using Dianthus caryophyllus WE.

Keywords: Dianthus caryophyllus, Nanoparticles, Antibacterial, Photocatalytic, Melamine adulteration, Cytotoxic.

1. Introduction

Nanoparticles are small molecules between 1 to 100 nanometers (nm) in size as shown below in figure 01 and are not visible to the naked eye.[1] They are also considered the elements of nanotechnology which is the research and development at a macromolecular scale. Electronic, magnetic, and optoelectronic, biological, pharmacological, cosmetic, energy, environmental, catalytic, and materials applications are just a few of the fields in which nanoscale materials are used.[2]

There are two approaches to the synthesis of nanoparticles namely bottom-up and top-down approaches. Both these approaches are shown below in figure 02. In the bottom-up approach, atoms or/and some molecular species interact to form nanomaterials through a series of chemical processes, and in the top-down approach an energy source is supplied, the beginning material,

which is a bulk form of the desired synthetic material, is subsequently broken into smaller and smaller pieces or particles.[4]

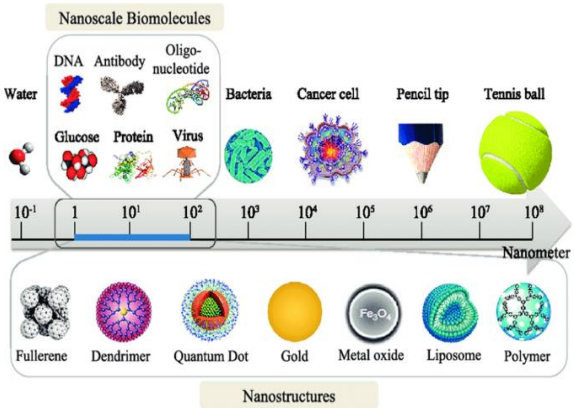

Figure 1. Nanoscale integration of nanoparticles.[3]

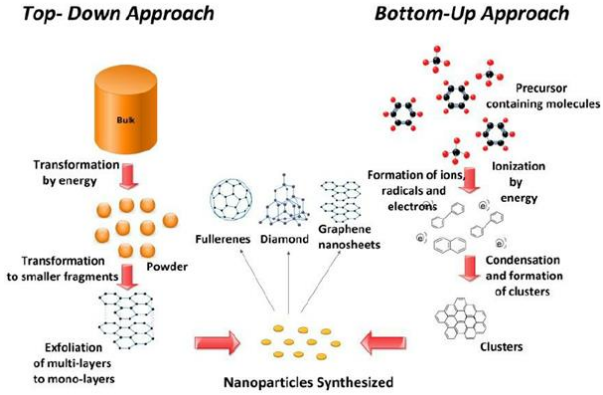

Figure 2. Bottom-up and top-down approaches.[4]

In comparison to chemical, physical, and microbiological approaches, the synthesis of metal nanoparticles using plant medicated techniques has several advantages. It is a quick, easily repeatable, ecological, and inexpensive process. Hence, using biological extracts from various plant components to create metal nanoparticles is widely encouraged.[5]

The sample used in this research is the leaves of 5 different *Dianthus caryophyllus* plants (figure 3). Research on the properties of the *Dianthus caryophyllus* leaves has not been done yet. But research on the flowers of *Dianthus caryophyllus* has been done and the phytochemical examination revealed that it included triterpenes, alkaloids, and many other chemical components. Pharmacological research also showed that the plant has anticancer, antiviral, antibacterial, antifungal, insecticidal, and antioxidant properties.[6]

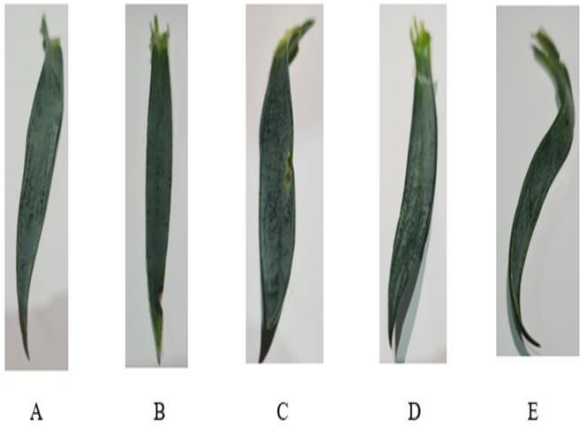

Figure 3. Variety of *Dianthus caryophyllus* used.

(A – Pink, B – Purple, C – White, D – Pink-White, E – Purple-White)

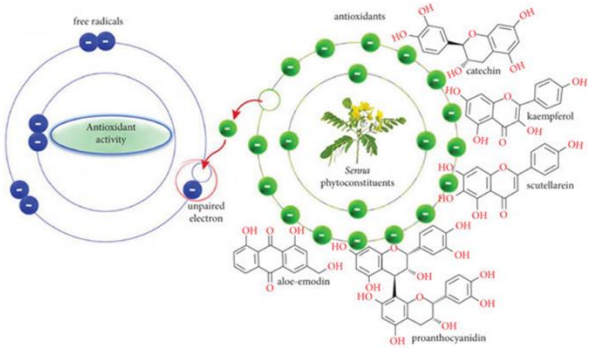

Figure 4. Antioxidant activity of bioactive compounds.[7]

Any substance that, when present in small amounts compared to an oxidizable substrate's concentrations delays or stops the oxidation of that substrate, is considered an antioxidant.[8] Figure 04 shows a brief overview of how that occurs. Antioxidants are classes of substances that stop free radicals and reactive oxygen species (ROS) from harming cells.[9] They are enzymes that fight off free radicals to

counteract any adverse effects that reactive oxygen and nitrogen species can have.[10] The ability to biosynthesize a variety of non-enzymatic antioxidants that can reduce reactive oxygen species-induced oxidative damage can be seen in plants therefore, it is more suitable for research that includes checking for antioxidant activity.[11] The development of many chronic diseases, including cardiovascular diseases, aging, heart disease, anemia, cancer, and inflammation, was significantly influenced by the presence of these antioxidants, which offer protection against the harm caused by free radicals.[9]

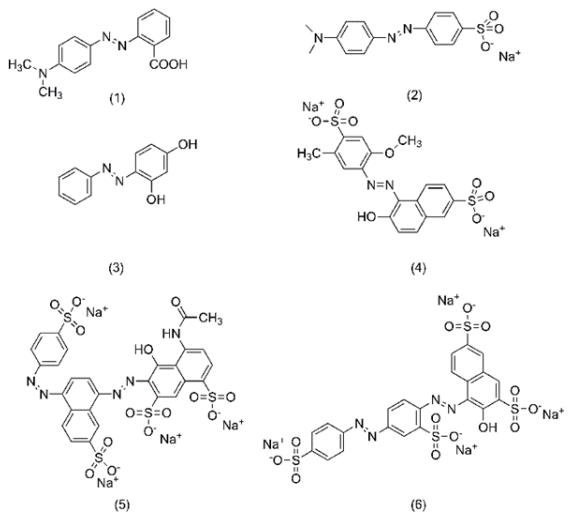

Figure 5. The azo dye structure in the following samples (1) methyl red (2) methyl orange (3) Sudan orange G (4) Allura red AC (5) Brilliant Black BN (6) Ponceau S.[12]

Before being released into the environment, organic substances found to be pollutants must be removed or destroyed.[13] By absorbing both visible and UV light from the sun spectrum, AgNPs are known to photo-catalytically break down these organic molecules like the dyes shown in Figure 05. Some azo dyes have been associated with hepatocarcinoma, splenic sarcomas, human cancer, nuclear anomalies in laboratory animals, and chromosomal abnormalities in mammalian cells.[14]

A molecule's antibacterial action is exclusively linked to substances that selectively kill the growth of bacteria without causing significant tissue damage in the surrounding area. The most crucial agents in the battle against infectious diseases are antibacterial ones.[15] The main mechanisms behind the antibacterial actions of AgNP's, according to current research, are as follows: Bacterial cell membrane disruption, ROS production, cell membrane penetration, and development of intracellular antibacterial effects, including interactions with deoxyribonucleic acid (DNA) and proteins.[16] Due to its potent biocidal impact against germs, which has been utilized for decades to prevent and treat a variety of diseases, AgNP's are well known as the most ubiquitous antimicrobial compounds.[17]

Milk is one of the best sources of the essential nutrients that both infants and adults need, including protein, fat, carbohydrates, vitamins, and minerals. Unfortunately, there is a problem with adulterated milk all throughout the world.[18] Milk is adulterated with melamine which is a synthetic chemical compound that has a high nitrogen concentration and has therefore been used to falsify the protein content of items containing protein, such as pet meals, milk, and newborn formula.[19] Kidney stones and renal failure can result from consuming this.[20] Because of their simple production, stability, and biocompatibility, AgNP's have been widely utilized for the detection of melamine. AgNP aggregates because of the interaction by hydrogen-bonding recognition, electrostatic interaction, or donor-acceptor contact, which causes a shifting of resonant excitation when melamine is added.

When identifying the potential toxicity of a test sample, such as plant extracts or physiologically active chemicals extracted from plants, cytotoxicity studies are helpful in the first step. For a pharmaceutical to be developed successfully, there must be little to no toxicity, and cellular toxicity studies are critical in this regard.[21]

The purpose of this study is to determine whether silver nanoparticles may be produced from the *Dianthus caryophyllus* leaves. Then, making use of TFC, TPC, TAC, and DPPH tests, to determine whether the AgNP's display strong antioxidant activity. Photocatalytic activity was tested using MR by leaving it under ultraviolet (UV) and sunlight (SL), a catalyst was used under SL. *E. coli* and *S. aureus* were used to test the antibacterial activities. AgNP's were tested to determine whether it could aid in melamine detection and using brine shrimps, cytotoxic evaluation was carried out.

2. Methodology

2.1 Water extract formation. The sample was shade dried for 2 weeks and then crushed using a mortar and pistol. It was then mixed with 50 milli liters (mL) of distilled water and incubated at 99°C for 20 minutes (mins). Then filtered off using Whatman filter paper 01, it was stored at 4°C for future use.

2.2 Phytochemical analysis. Water extracts were used for this analysis (table 2).

Table 2. Phytochemical analysis.

Test	**Procedure**
Saponins	To 0.5mL of water extract, 3 drops of distilled water was added and was shaken for a few minutes.[22]
Tannins	To 0.5mL of water extract, 0.8mL of distilled water was added along with 2 drops of 0.1% Ferric chloride.[22]
Sterols and Triterpenoids	To 0.5mL of water extract, 3 drops of Conc. Sulfuric acid was added and shaken well.[22]
Carbohydrates	To 0.5mL of water extract, 3 drops of molish reagent was added, then along the wall of the test tube, Conc Sulfuric acid (H_2SO_4) was added.[23]
Amino Acids	To 0.5mL of water extract, 5 drops of Ninhydrin was added, and the test tube was heated until it boiled.[23]
Alkaloids	To 0.5mL of water extract, 3 drops of Conc HCl and 3 drops of Mayers reagent was added.[23]

2.3 Synthesis of silver nanoparticles. 1mL of the water extract was mixed with 9mL of 1 milli molar (mM) silver nitrate solution and incubated at 60°C and 90°C for 15,30,45 and 60mins and at 25°C for 24hrs. They were then stored at 4°C until they were used.

2.4 Characteristics of AgNP's. Using the spectrophotometer, the absorbance rates was taken from 340-520nm. An SEM analysis was also carried out by centrifuging the AgNP's at 5000rpm for 2mins and incubating for 24hrs at 40°C. The pellet was then outsourced to SLINTECH for analysis where the Hitachi SU6600 FE-SEM (Field Emission Scanning Electron Microscope) and Oxford instruments EDX with AZtec software was used.

2.5 Dilution of Water Extract and Nanoparticles. 1mL of the sample was diluted ×15 times with distilled water and was used for the assays below.

2.6 Antioxidant assessment. WE and AgNP's were both used in these assays (table 3), and they were performed in triplicates.

Table 3. Assays for antioxidant assessment.

Total Flavonoids Content	To 1mL of the sample, 0.5 mL of 1% Aluminum Chloride ($AlCl_3$) and 0.5 mL of 1mM Potassium Acetate were added. Reading was taken at 415nm.[24] Quercetin standard curve was used to get the TFC value, and it was expressed in (µg QE/100g).
Total Phenol Content	To 125µL of a sample, 125µL of 10% Folin – Ciocalteu reagent and 2mL of 5% Sodium Carbonate (Na_2CO_3) were added and incubated at room temperature in the dark for 1 and half hours. Reading was taken at 760nm.[25] Gallic acid standard curve was used to get the TFC value, and it was expressed in (g GAE/100g).
Total Antioxidant Capacity	To 300µL of sample 2.7mL of the mixture of equal volume of 30mL 4mM Ammonium Molybdate, 30mL 28mM Sodium Phosphate, and 30mL 0.6M H_2SO_4 was added. Reading was taken at 630nm.[24] Ascorbic acid standard curve was used to get the TFC value, and it was expressed in (g AAE/100g).

2.6.1. 2,2-diphenyl-1-picryl-hydrazyl-hydrate (DPPH) assay. A ×15 dilution of the AgNP's and WE's was prepared. 1mL of the sample was added to 1mL of 0.135mM DPPH. Readings were taken at 517nm at 0mins and 30mins.[26] Percentage activity was then calculated using equation 01.

Equation 01.

$$Percentage\ activity = \frac{Absorbance\ of\ DPPH - 100\%\ absorbance}{Absorbance\ of\ DPPH} \times 100$$

2.7 Photocatalytic assessment

2.7.1. Degradation MR using UV light. To 100mL of 1mM of MR dye, 1mL of 4000ppm pink-AgNP was added and kept in UV light. Readings were taken from 300-600nm every hour for 4 hours. The same procedure was carried out for 267ppm.[27]

2.7.2. Degradation of MR dye using sunlight. The same procedure as 2.7.1 was repeated with Sunlight. Readings were taken from 300-600nm every hour for 4 hours.[27]

2.7.3. Degradation of MR using sodium borohydride ($NaBH_4$) *and sunlight.* The same procedure as 2.7.1 was repeated including 1mL of 0.2M $NaBH_4$ and sunlight. Readings were then taken from 300-600nm every 15mins for 2.5 hours.[27]

2.8 Detection of melamine

2.8.1. Detection of melamine with AgNP. A series of melamine concentrations from 1000ppm, 100ppm, 10ppm, 1ppm, and 0.1 ppm were prepared. 400µL of melamine was mixed with 600µL of pink-AgNP. Readings were then taken at times o minute and time 30 minutes from wavelength 340-720nm.[28]

2.8.2. Detection of melamine in milk with AgNP. 20mL of milk was heated until it reached 90°C, and it was then cooled until it reached 60°C. 25 drops of citric acid were then added, and the mixture was centrifuged at 4000ppm for 45mins. The milk was then filtered, and the supernatant was collected. 600µL of the milk supernatant, 800µL of pink AgNP and 600µL of 1ppm melamine were mixed. Separately 600µL of the milk supernatant, and 800µL of pink-AgNP were also mixed and used. Readings were then taken at

times 0 minute and time 30 minutes from wavelength 340-720nm.[28]

2.8.3. Detection of melamine using WE and $AgNO_3$. The same series of melamine concentrations as 2.8.1 was used. 2000µL of $AgNO_3$, 40µL of pink-WE, and 800µL of melamine were mixed and incubated at 60°C for 1 hour. Readings were then taken from 340-720nm.[28]

2.8.4. Detection of melamine in milk with WE and $AgNO_3$. 20mL of milk was heated until it reached 90°C, and it was then cooled until it reached 60°C. 25 drops of citric acid were then added, and the mixture was centrifuged at 4000ppm for 45mins. The milk was then filtered, and the supernatant was collected. 800µL of the milk supernatant, 2mL of silver nitrate, 40µL of pink-WE and 800µL of 1ppm melamine were mixed. Separately 800µL of the milk supernatant, 2mL of silver nitrate, and 40µL of pink-WE were also mixed and used. They were both incubated at 60°C for 1hr. Readings were taken from 340-720nm.[28]

2.9 Antibacterial assessment. Agar was prepared by boiling the agar and distilled water and then autoclaving it. 1mL of the sample was incubated at 40°C until it evaporated. The Petri plates containing agar were streaked with *E. coli* and *S. aureus* respectively and then prepared as shown below by adding small wells in which respective samples were added as shown in figure 07. It was then incubated at 37°C for 24hrs and the zone of inhibition was checked.[29]

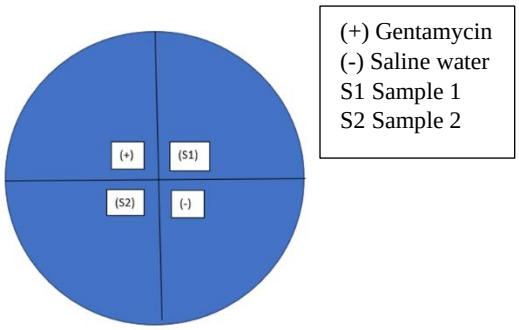

Figure 7. Illustration of the Petri plates.

2.10 Cytotoxic assessment. Capsulated brine shrimp were grown in sea water for 24hrs. Two dilutions of 40mg/ml and 10mg/ml of the pink-AgNP sample were made. Into 25 wells of the 96 well plate, 200µL of sample and 2 shrimps were added and left for 24hrs under the yellow light. 5 wells were used as a control where only sea water and shrimps were added.[30]

2.11 Statistical analysis. The obtained results were analyzed using one-way ANOVA using Microsoft excel and Pearson's correlation test to determine the correlation of TAC TPC and TFC.

3. Results

3.1 Phytochemical analysis. Water extracts were used for the Phytochemical test.

Table 4. Phytochemical results.

Phytochemicals	Pink	Purple	White	Pink & White	Purple & White
Saponins	✓	✓	✓	✓	✓
Tannins	×	×	×	×	×
Sterols	×	×	×	×	×
Triterpenoids	✓	✓	✓	✓	✓
Carbohydrates	✓	✓	✓	✓	✓
Amino Acids	✓	✓	✓	✓	✓
Alkaloids	×	×	×	✓	×

3.2 Silver Nanoparticles

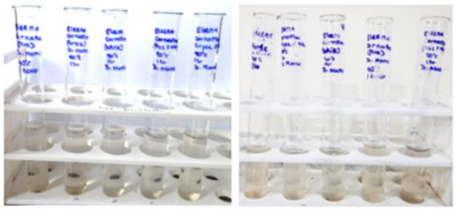

Figure 8. Before and After incubation at 60°C for 1 hour.

A slight cloudy appearance can be seen after incubation.

3.3 Silver nanoparticles graph

Peaks can be seen near 480nm. This confirms the presence of nanoparticles.

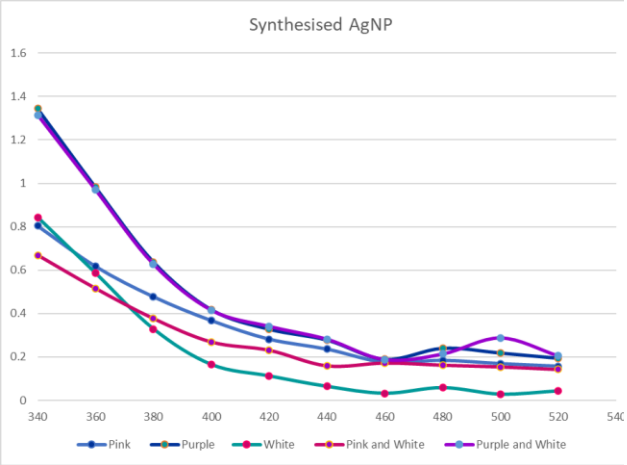

Figure 9. Graph showing nanoparticle peak.

3.4 Optimization table of AgNP synthesis

Table 5. Optimization table of the silver nanoparticles.

Temp	Time	Pink	Purple	White	Pink-White	Purple-White
90°C	1hr	✗	✗	✗	✗	✓
	45mins	✗	✗	✓	✓	✗
	30mins	✗	✗	✓	✗	✗
	15mins	✓	✗	✗	✓	✗
60°C	1hr	✓	✓	✓	✓	✓
	45mins	✗	✓	✓	✗	✗
	30mins	✗	✗	✓	✗	✗
	15mins	✗	✗	✗	✓	✓
25°C	24hrs	✗	✓	✓	✗	✗

The optimized samples are highlighted on table 5.

3.5 SEM Analysis

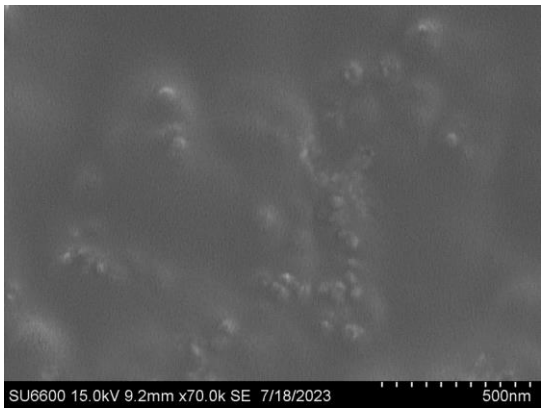

Figure 10. SEM image of pink-AgNP 15kV 9.2mm x70 k/scale - 500nm

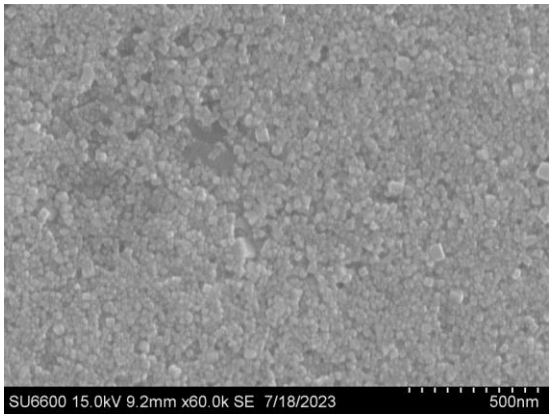

Figure 11. SEM image of pink-AgNP 15kV 9.2mm x60 k/scale -500 nm

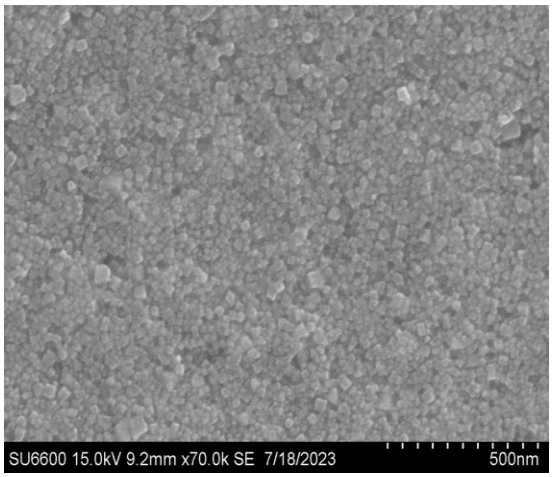

Figure 12. SEM image of pink-AgNP 15kV 9.2mm x70 k/scale - 500nm

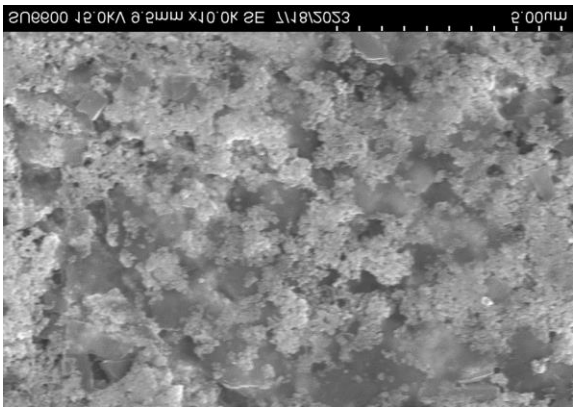

Figure 13. SEM image of pink-AgNP 15kV 9.5mm x10 k/scale - 5µm

The pink-AgNP is cuboidal in shape and has a size of around 50nm.

3.6 Total Flavonoid Content

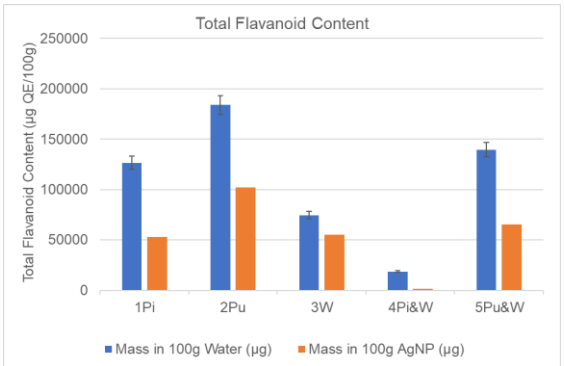

Figure 14. TFC of WE's and AgNP's.

Water Extract has a higher TFC level than AgNPs.

Table 6. ANOVA test for TFC

ANOVA						
Source of Variation	*SS*	*df*	*MS*	*F*	*P-value*	*F crit*
Between Groups	6164560200	1	6.16E+09	2.012153	0.198403	5.591448
Within Groups	21381886800	7	3.05E+09			
Total	27546447000	8				

The P value is 0.198403 which is higher than the significant value 0.05.

3.7 Total Phenol Content

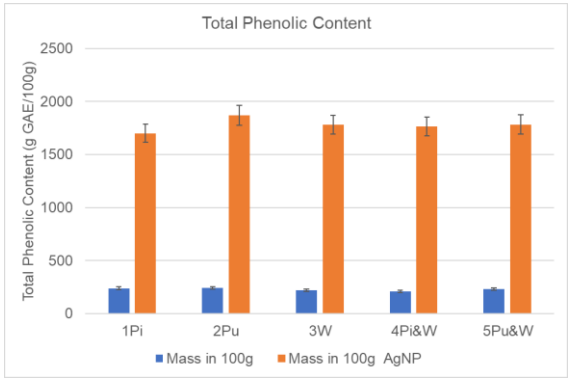

Figure 15. TPC of WE's and AgNP's.

AgNP has a higher TFC level than WE.

Table 7. ANOVA for TPC

ANOVA						
Source of Variation	*SS*	*df*	*MS*	*F*	*P-value*	*F crit*
Between Groups	5481045	1	5481045	5163.164	2.65913E-11	5.591448
Within Groups	7430.969388	7	1061.567			
Total	5488475.969	8				

The P value is 2.65913E-11 which is lower than the significant value 0.05.

3.8 Total Antioxidant Activity

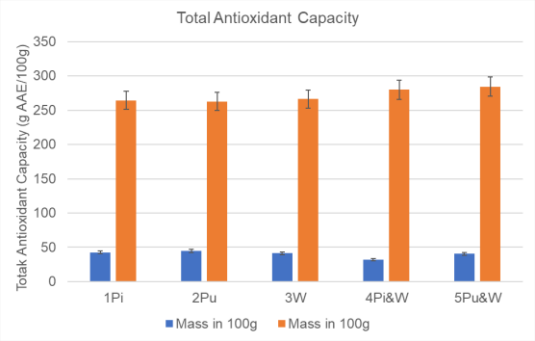

Figure 16. TAC of WE and AgNP's.

AgNP has a higher TAC level than WE.

Table 8. ANOVA for TAC

ANOVA						
Source of Variation	*SS*	*df*	*MS*	*F*	*P-value*	*F crit*
Between Groups	120736.382	1	120736.4	2023.084	7.02E-10	5.591448
Within Groups	417.7556818	7	59.67938			
Total	121154.1377	8				

The P value is 7.02E-10 which is lower than the significant value 0.05.

3.9 DPPH Activity

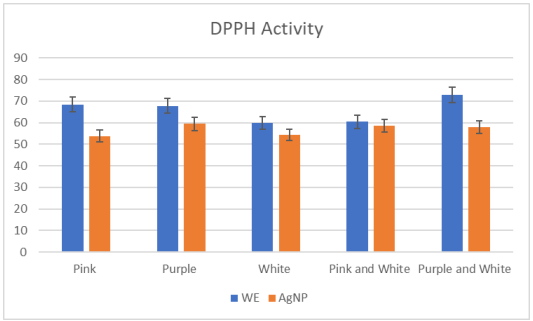

Figure 17. DPPH activity of WE and AgNP

WE's have more DPPH activity than AgNP's.

3.10 Photocatalytic of AgNP.

3.10.1 Under UV using pink-AgNP.

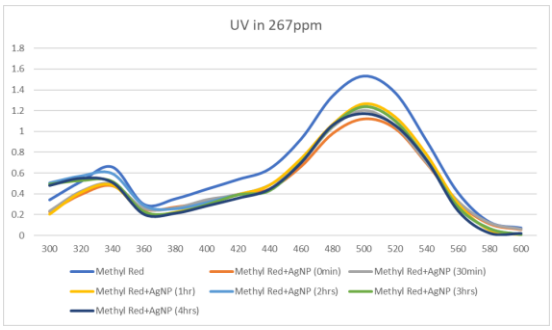

Figure 18. Photocatalytic activity of MR in the presence of 267ppm *pink-AgNP* under UV.

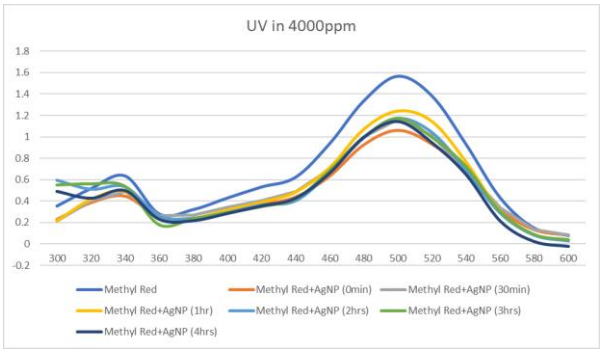

Figure 19. Photocatalytic activity of MR in the presence of 4000ppm *pink-AgNP* under UV.

There is no degradation seen under UV as shown in figures 18 and 19.

3.10.2 Under Sunlight using pink-AgNP.

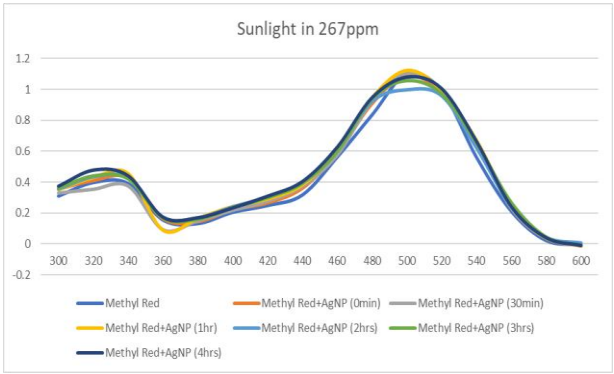

Figure 20. Photocatalytic activity of MR in the presence of 267ppm *pink-AgNP* under sunlight.

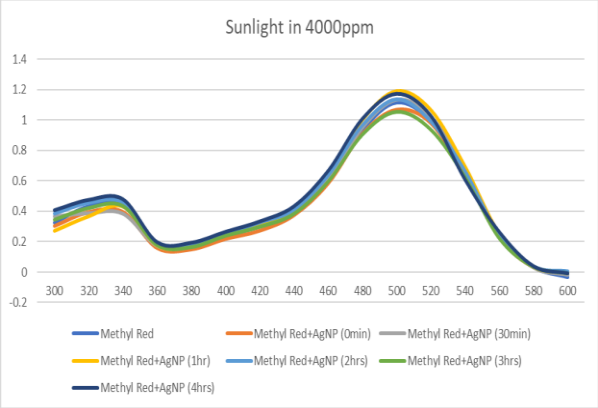

Figure 21. Photocatalytic activity of MR in the presence of 4000ppm *pink-AgNP* under sunlight.

There is no degradation seen under SL as shown in figure 20 and 21.

3.10.3 Under Sunlight with $NaBH_4$ using pink-AgNP.

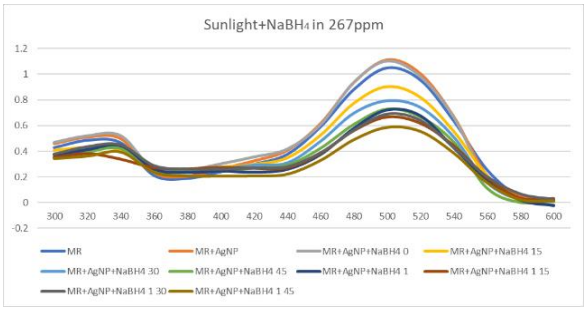

Figure 22. Photocatalytic activity of MR in the presence of 267ppm *pink-AgNP* and $NaBH_4$ under sunlight.

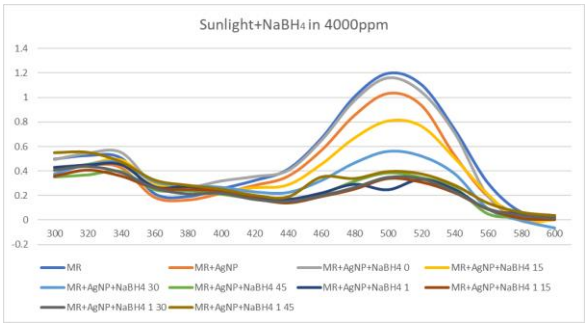

Figure 23. Photocatalytic activity of MR in the presence of 4000ppm *pink-AgNP* and $NaBH_4$ under sunlight.

Degradation of MR is shown in figure 23. The curve became flat at 1 hour and 45mins.

3.11 Melamine detection.

3.11.1 Detection of melamine with pink-AgNP.

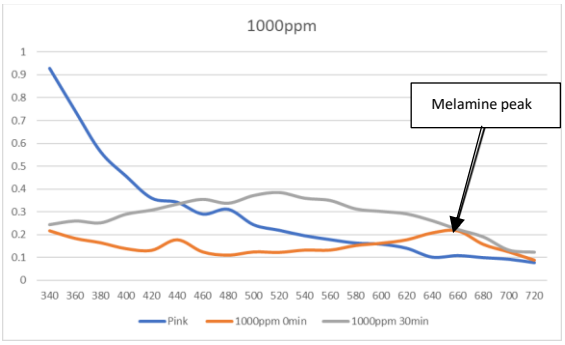

Figure 24. Melamine detection with 1000ppm pink-AgNP.

The peaks are seen near 640nm.

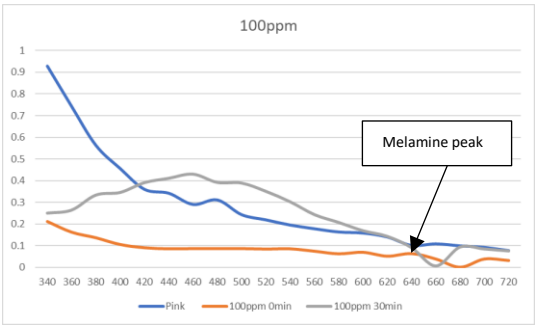

Figure 25. Melamine detection with 100ppm pink-AgNP.

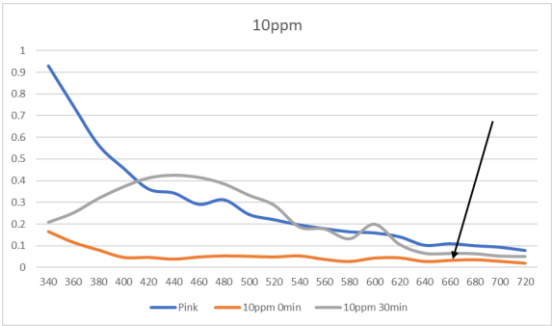

Figure 26. Melamine detection with 10ppm pink-AgNP.

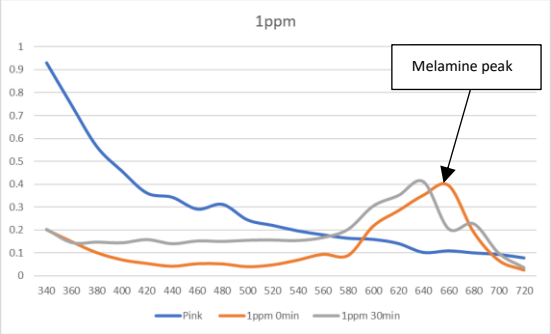

Figure 27. Melamine detection with 1ppm pink-AgNP.

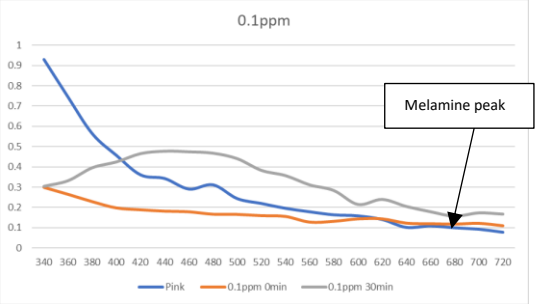

Figure 28. Melamine detection with 0.1ppm pink-AgNP.

Melamine was detected in all concentrations using this method.

3.11.2 Detection of melamine with pink-WE and $AgNO_3$

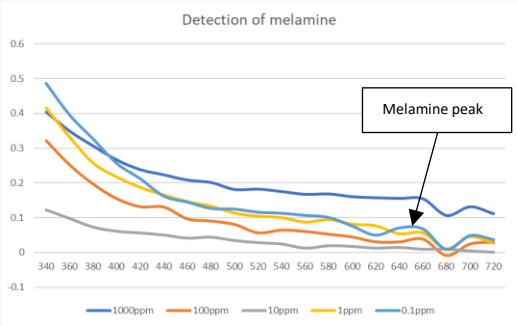

Figure 29. Melamine detection with pink-WE and $AgNO_3$.

Melamine was detected in all concentrations except 1000ppm.

3.11.3 Detection of melamine in milk with pink-WE & $AgNO_3$.

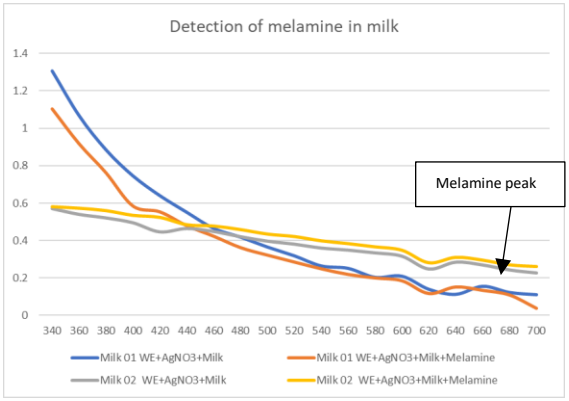

Figure 30. Melamine detection in 2 different milk samples with pink-WE and $AgNO_3$.

Melamine was detected in both milk samples.

3.12 Antibacterial assessment

Table 9. Zone of inhibition (ZOI) for *S. aureus* using WE & AgNP

Sample	**S1**	**S2**	**(+) ve control**
Pink WE	-	-	2.3cm
Purple WE	-	-	2.3cm
White WE	-	-	2.3cm
Pink-White WE	-	-	2.3cm
Purple-White WE	-	-	2.3cm
Pink AgNP	-	-	2.3cm
Purple AgNP	-	-	2.2cm
White AgNP	-	-	2.2cm
Pink-White AgNP	1.2cm	1.0cm	2.3cm
Purple-White AgNP	-	-	2.3cm

Table 10. ZOI for *E. coli* using WE & AgNP

Sample	S1	S2	(+) ve control
Pink WE	-	-	2cm
Purple WE	-	-	2cm
White WE	-	-	2cm
Pink-White WE	-	-	2cm
Purple-White WE	-	-	2cm
Pink AgNP	-	-	2cm
Purple AgNP	-	-	2cm
White AgNP	0.8cm	0.8cm	2cm
Pink-White AgNP	-	-	2cm
Purple-White AgNP	-	-	2cm

Pink-white AgNP showed a ZOI when *S. aureus* was used while the white AgNP showed a ZOI when *E.coli* was used.

3.13 Cytotoxic assessment

Control

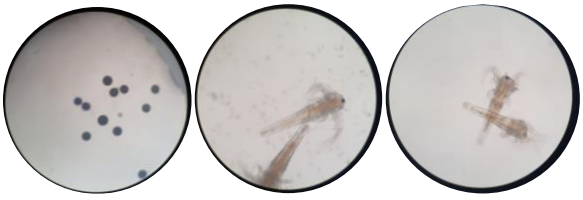

Eggs Hatchlings After 24hrs

10mg/L

Eggs Hatchlings 24hrs after AgNP

40mg/L

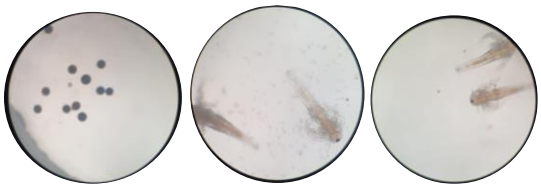

Eggs Hatchlings 24hrs after AgNP

Figure 31. Cytotoxic assessment using pink-AgNP.

After 24 hours all 50 shrimps used in the test were alive. Microscopic imaging can be seen (Figure 33).

4. Discussion

In this study silver nanoparticles were synthesized using leaves of 5 varieties of *Dianthus caryophyllus* flowers. This was used to check for antioxidant, photocatalytic, antibacterial, and cytotoxic activity as well as melamine adulteration in milk. In this study, the WE were synthesized by incubating the water and leaf mixture at 99°C for 1 hour, this was then mixed with AgNO3 and incubated at 60°C for 1 hour. The confirmation of the nanoparticles was done by using the spectrophotometer where a peak was seen at 480nm, as shown in figure 9, this was also confirmed using the research by Aisida *et al*., (2019) where it states that the specific surface plasmon resonance absorption peaked between 450 - 480nm.[31] A change in color was not easily observed as seen in figure 8 as the transparent mixture turned slightly cloudy white which could be due to the presence of many silver nanoparticles which give a grey and white.[32]

Among the several metallic nanoparticles used in biomedical applications, AgNP's are one of the most important and fascinating nanomaterials. They also play a crucial part in nanomedicine and nanoscience.[33] Since AgNP's are widely used for many different applications, it is inevitable that they will end up in environmental systems. Therefore, it is crucial

that research is done on AgNP's characteristics.[34] AgNP's can be easily synthesized using physical, chemical, and biological techniques. As a result of their high surface-to-volume ratio and exceptional conductivity, they have found extensive usage in chemistry and related fields.[35] Research on AgNP's is made simple due to their flexibility, which allows for their simple incorporation into a variety of media.[36]

Further analysis was carried out to check for the size and shape of the AgNP. According to the analysis, (figures 10-13) it can be confirmed that the AgNP is cuboidal in shape and is around 50nm in size.

Table 11. Confirming for the conductivity of optimized samples.

Purple	4.14E-19	2.584968	Semiconductors
White	4.14E-19	2.584968	Semiconductors
Pink & White	4.32E-19	2.697358	Semiconductors
Purple & White	4.14E-19	2.584968	Semiconductors

Equation 02.

$$\text{Conductivity equation} = \text{Plank's constant} \times \frac{\text{speed of light}}{\text{Peak wavelength}}$$

The results seen in table 11 were obtained using equation 2, this confirmed that all four AgNP samples show semiconductive properties.

The results of the phytochemical analysis seen in table 4 confirmed the presence of saponins, triterpenoids, carbohydrates, amino acids, and alkaloids which is supported using the research by Chandra and Rawat (2015) which mentions that *Dianthus caryophyllus* consists of significant levels of secondary metabolites.[37]

By indirectly increasing the activity of intracellular antioxidant enzymes or directly by interacting with free radicals, antioxidants are known to reduce oxidative damage.[38]

The TFC of the WE and the AgNP's were carried out using aluminum chloride and potassium acetate. As shown in Figure 34, the basic principle of this assay suggests that aluminum chloride forms stable acid complexes with C-4 keto groups and either C-3 or C-5 hydroxyl groups of flavones and flavanols.[40] The results (figure 14), state that purple WE have the highest levels of TFC while pink-white WE have the lowest level, and this was similar to the AgNP's. This finding is also further confirmed by the research carried out by Zhou *et al*., (2023) which suggests that the purple *Dianthus caryophyllus* WE have higher levels of flavonoids.[41] According to the results WE have a higher TFC level than AgNP's. The p–value is > than the significant value, and the F value< F crit value (table 6), therefore it can be concluded that there is no statical significant between the TFC activity of WE's and AgNP's (table 6).

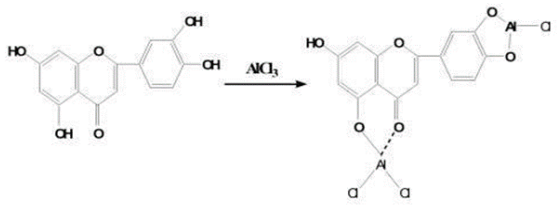

Figure 32. Principle of TFC.[39]

The TPC of the WE and AgNP's were carried out using folin – ciocalteu reagent. The production of a blue compound, which is detected at a wavelength of 765 nm, is the fundamental idea behind this technique. The heteropoly acid (phosphomolybdate-phosphotungstate) included in the folin-ciocalteau reagent will be oxidised by phenol or phenolic-hydroxy groups to produce a molybdenum-tungsten complex which is seen in Figure 35.[43] According to figure 15 the AgNP's

have higher activity than the WE, this is supported by research done by Gonçalves *et al*., (2020) confirming the presence of high penolic content in AgNP.[25] The p–value is < than the significant value, and the F value > F crit value (table 7), therefore it can be concluded that there is a statistical significance between the TPC activity of the WE's and AgNP's.

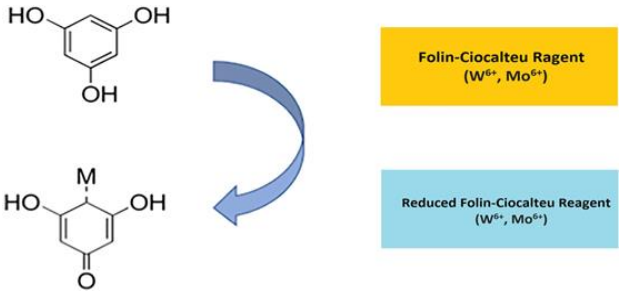

Figure 33. Principle of TPC.[42]

The TAC was carried out using phosphomolybdenum assay. As shown in Figure 36, Mo (VI) is converted to Mo (V) in the presence of extracts, forming phosphomolybdenum V complex, this is green in color and has a with a maximum absorbance at 695 nm.[45] The result (figure 16) states that AgNP's have higher TAC activity than the WE, the research by Ioana-Raluca Bunghez *et al*., (2012) supports this as it states that compared to plant extract, all silver nanoparticles displayed higher antioxidant activity levels.[46] The p–value is < than the significant value, and the F value > F crit value (table 8), therefore it can be concluded that there is a statistical significance between TAC activity of WE and AgNP's.

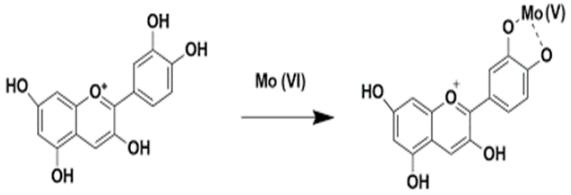

Figure 34. Principle of TAC.[44]

The accepted correlation measure in statistics is the Pearson Correlation, this displays the linear relationship between the two sets of data, and is the most popular technique for analyzing numerical variables.[47] It works by assigning a value between 0 and 1, with 1 denoting total positive correlation and 0 denoting total negative correlation.[48] The results (figure 37) concluded that there is no statistical relationship between TFC-TPC, and between TFC-TAC. But there is a statistical relationship between TPC-TAC.

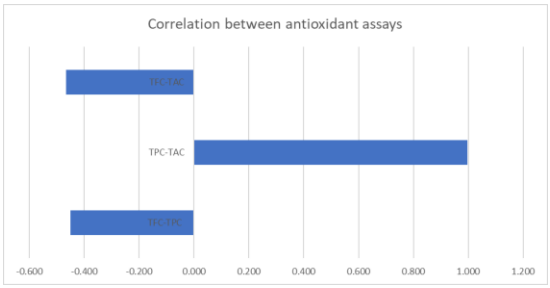

Figure 35. Correlation between antioxidant assays.

The DPPH assay was carried out to determine the free radicle scavenging activity of the WE's and AgNP's. The DPPH radical is a stable, methanol-soluble molecule with a deep violet color and a maximum absorption wavelength of 515 nm. By providing an electron or hydrogen atom, antioxidants can react with this stable radical, reducing it to 2,2-diphenyl-1-hydrazine (DPPH-H) or a substituted analogous hydrazine (DPPH-R), which is colorless or has a pale-yellow appearance, this can be easily observed using a spectrophotometer.[49] The results in figure 17 indicated that the WE's have better activity than the AgNP's, this is supported using the research by Zia *et al*., (2019) which states that low free radical scavenging activity is correlated with higher phenolic levels and overall antioxidant activity.[24]

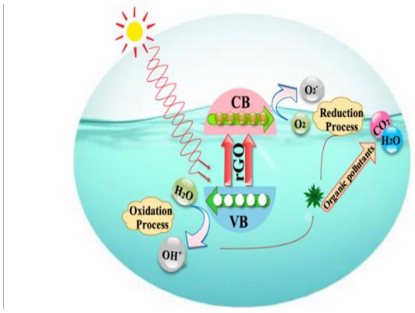

Figure 36. Photocatalytic mechanism for dye degradation.[50]

AgNP's ability to absorb UV energy from the solar spectrum results in the excitation of electrons from the 4d orbital to the 5sp orbital. Numerous photogenerated electrons are excited due to this interband transition. The oxygen molecules and the hydroxyl ion are both affected by these excited electrons, resulting in the formation of oxygen radicals and hydroxyl radicals as shown in figure 38. The dye is degraded because of radicals' attack on the dye molecule adsorbed on the surface of the AgNP's. In addition to the radicals' breakdown of the dyes, the holes created in the AgNP's d orbital take electrons from the dye molecule that has been adsorbed, further degrading the dye.[51] Confirming the photocatalytic activity of the AgNP's was carried out using the dye MR which is a synthetic azo dye that was discovered to be both mutagenic and to have serious negative effects on human health.[52] A UV spectrophotometer was used to confirm the findings and a peak was seen at 500-520nm this is confirmed using the research by Xu (2021) which stated that MR aqueous solution's UV-visible electronic absorption spectra are distinguished by the overlap of a major peak at 520±15nm.[53] The results obtained in figures 18-21, under UV and sunlight showed no significant decrease. Figures 22 and 23 illustrate how the addition of a catalyst under SL reduced the peaks; 267 ppm pink-AgNP showed less reduction than 4000 ppm pink-AgNP which resulted in a flat peak at 1 hour and 45 minutes. This is confirmed using research by Kansal *et al*., (2007) that stated that degradation of dye with the help of metal catalysts in the presence of sunlight was faster compared to other irradiation techniques.[54] Githala *et al.,* (2022) also confirmed that high concentrations of AgNP's with the help of $NaBH_4$ show full degradation of the dye molecules.[55] According to the rate constant was calculated (figures 39 and 40), the concentrated sample of 4000ppm pink-AgNP has a rate constant of 0.0709 while the diluted sample of 267ppm pink-AgNP has a rate constant of 0.0326 this confirms the concentrated sample has a faster rate of degradation than the diluted sample.

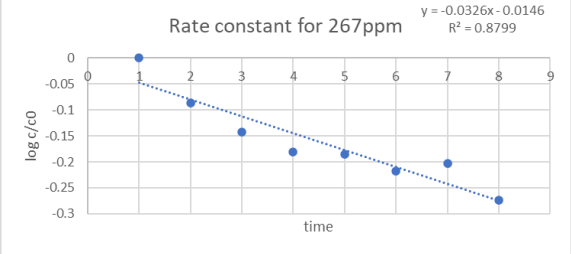

Figure 37. Rate constant for MR under SL with $NaBH_4$ at 267ppm.

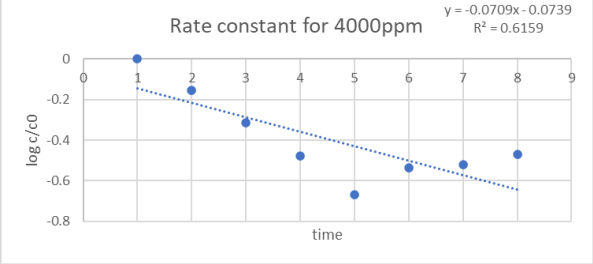

Figure 38. Rate constant for MR under SL with $NaBH_4$ at 267ppm.

Melamine detection is important to reduce melamine adulteration in milk as they cause harm to the human body. A spectrophotometer is used to confirm the findings, the melamine peaks are seen between 600-640nm this was confirmed using the research by Siddiquee *et al*., (2021) which stated that the emergence of a new absorption peak at about 600 nm was induced by melamine.[56] The

nanoparticles engage through hydrogen-bonding recognition, electrostatic interaction, or donor-acceptor interaction, and cause the nanoparticles to aggregate. Melamine's addition causes the resonant excitation to shift, which causes the solution's color to shift from bright yellow to pale red.[38] Melamine was detected in all concentrations (1000ppm, 100ppm, 10ppm 1ppm and 0.1ppm) when pink-AgNP's were used (figures 24-28). Whereas when another method was carried out by adding WE's and $AgNO_3$, melamine was not detected in 1000ppm (figure 29). The research by Ramalingam *et al*., (2017) suggested that absorbance decreases as melamine concentration increases which supports the results obtained.[57] Melamine was detected in two samples of milk, both of which showed melamine peaks as seen in figure 30. This indicated that both these milk samples are adulterated with melamine and could potentially cause harm to the people.

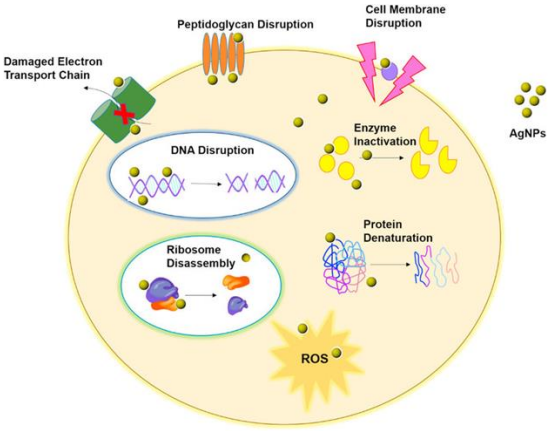

Figure 39. The mechanism of antibacterial activity of silver nanoparticles.[58]

The AgNP adhesion to the microbial cell wall and membrane along with the electrostatic attraction between the negatively charged microbial cell membrane and positively charged AgNP's as seen in figure 41 is the first step in the interaction between AgNP's and microbes. Following the interaction, the nanoparticle causes morphological changes in the membrane structure, which impair membrane permeability and respiratory processes via membrane depolarization, and ultimately destroy cell integrity and cause cell death. Proteins, enzymes, DNA, ions, metabolites, and the energy reserve all leak out of cells into the environment because of increased membrane permeability and damage to the cell wall. Thus, it is considered that the major mechanism of the antibacterial effect is the breakdown of the cell wall by the attachment of nanoparticles.[59] Antibacterial activity of the WE and the AgNPs was carried out using *E. coli* and *S. aureus*. Results were seen for the pink-white AgNP using *S. aureus* and the white AgNP using *E. coli*. Tables 9-10 presented the diameter of the zone of inhibition, this confirmed that AgNP's have better antibacterial activity than WE's.

The brine shrimp were used to test the cytotoxicity of the pink-AgNP's. They developed in a lab with saltwater, yellow light and algae food, and a 24-hour maturation period before being subjected to the test. They are used in this research since they are inexpensive, easy to handle, and needed in limited numbers.[60]

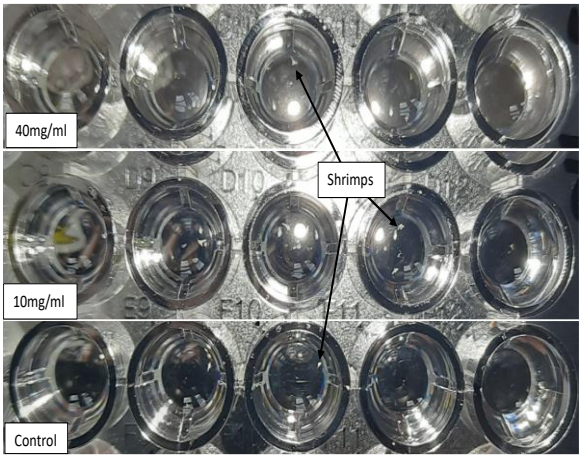

Figure 40. 96 well plates with the shrimps.

The shrimps were added in the same manner as figure 42. The percentage viability of the shrimps was obtained using equation 3, this confirmed the shrimps showed 100% viability 24 hours after the addition of the pink-AgNP. Therefore, it can be concluded that the pink-AgNP sample is nontoxic.

Equation 03.

$$\text{Percentage viablility} = \frac{\text{No of viable shrimps} - \text{No of non viable shrimps}}{\text{No of viable shrimps}} \times 100$$

5. Conclusion

In conclusion, five optimized AgNP's samples were synthesized, the optimized AgNP samples were synthesized by incubation at 60°C for 1hour. Higher TFC and DPPH results were seen in WE, while higher TPC and TAC results were seen in AgNP. When $NaBH_4$ was utilized dye degradation was visible, however it was not visible under UV and SL. AgNP allowed for the detection of melamine at all 5 concentrations (1000ppm, 100ppm, 10ppm, 1ppm and 0.1ppm), however detection via the addition of WE and $AgNO_3$ was not successful at 1000ppm, melamine was also detected in two milk samples. When *S. aureus* was used, the pink-white AgNP displayed antibacterial activity, and when *E. coli* was used, the white AgNP displayed antibacterial activity, 100% viability was also seen in the pink-AgNP. All these results indicated that the sample has high antioxidant activity, photocatalytic activity, antibacterial activity and can be very useful in the detection of melamine. This sample is also non-toxic as it showed 100% viability of the brine shrimps when AgNP's were added.

Acknowledgements

Authors thank BMS for funding.

References

1. R.W. Whatmore. *Occupational Medicin*, 2006;**56**(5);295-299.
2. P. Biswas and C.Y. Wu. *Journal of the Air & Waste Management Association*, 2005;**55**(6);708–746.
3. S. Saallah and I.W. Lenggoro. *KONA Powder and Particle Journal*, 2018;**35**;89-111.
4. K. Habiba, V. Makarov, B. Weiner and G. Morell. *Manufacturing Nanostructures*, 2014;263-291.
5. Rónavári, N. Igaz, D.I. Adamecz, B. Szerencsés, C. Molnar, Z. Kónya, I. Pfeiffer and M. Kirics. *Molecules*, 2021;**26**(4);844.
6. A.E. Al-Snafi. *IOSR Journal of Pharmacy (IOSRPHR)*, 2017;**7**(3);61-71.
7. M.M. Alshehri, C. Quispe, C, J. Herrera-Bravo, J. Sharifi-Rad, S. Tutuncu, E.F. Aydar, C. Topkaya, Z. Mertdinc, B. Ozcelik, M. Aital, N.V.A. Kumar, N. Lapava, J. Rajkovic, A. Ertani, S. Nicola, P. Semwal, S. Painuli, C. González-Contreras, M. Martorell, M. Butnariu, I.C. Bagiu, R.V. Bagiu, M.D. Barbhai, M. Kumar, S.D. Daştan, D.Calina and W.C. Cho. *Oxidative Medicine and Cellular Longevity*; 2022;**2022**;36.
8. B. Halliwell. *Advances in Pharmacology*, 1997;**38**(3);3-20.
9. C. Zehiroglu and S.B.O. Sarikaya. *Journal of food science and technology*, 2019;**56**(11);4757–4774.
10. Hunyadi. *Medicinal Research Reviews*, 2019;**39**(6);2505-2533.
11. D.M. Kasote, S.S. Katyare, M.V. Hegde and H. Bae. *International Journal of Biological Sciences*, 2015;**11**(8);982-991.
A. Ngo, F. Peter, A. Maier, S. Niklas and D. Tischler. *Chemistry Europe*, 2022;**23**(6).
12. P.G. Krishna, P.C. Mishra, M.M. Naika, M. Gadewar, P.P. Ananthaswamy, S. Rao, S.R.B. Prabhu, K.V. Yatish, H.G. Nagendra, M. Moustafa, M. Al-Shehri, S.K. Jha, B. Lal and S.M.S Santhakumari. *Frontiers in Chemistry*, 2022;**10**;2296-2646.
13. K. Shah. *International Research Journal of Biochemistry and Biotechnology*, 2014;**1**(2);5-13.
14. K. Singh, A. Mishra, D. Sharma and K. Singh. *Micro and Nano Technologies*, 2019;343–356.
15. L.L. Wang, C. Hu and L. Shao. *International Journal of Nanomedicine*, 2016;**12**;1227–1249.
16. Y.Y. Loo, Y. Rukayadi, M.A.R. Nor-Khaizura, C.H. Kuan, B.W. Chieng, M. Nishibuchi and S. Radu. *Frontiers Microbiology*, 2018;9.
17. M. Jalili. *Journal of Dairy & Veterinary Sciences*, 2017;**1**(4).
18. N. Kumar, H. Kumar, B. Mann, and R. Seth. *Spectrochimica Acta Part A: Molecular and Biomolecular Spectroscopy*, 2016;**5**;89-97.
19. S. Varun, S.C.G.K. Daniel and S.S. Gorthi. *Materials Science and Engineering: C*, 2017;**74**;253-258.
20. L.J. McGaw, E.E. Elgorashi and J.N. Eloff. *Toxicological Survey of African Medicinal Plants*, 2014;181–233.
21. M. Gupta, S. Thakur, A. Sharma and S. Gupta. *Oriental Journal of Chemistry*, 2013;**29**(2);475–481.
22. S.K. Manoharan, S.K. Sivagnanam, M.R.K. Rao and S. Anbuselv. *Asian Journal of Plant Science and Research*, 2013;**3**(43-46);43–46.
23. M. Zia, K. Yaqoob, A. Mannan, S. Nisa, G. Raza and R. Rehman. *Vegetos*, 2019;**33**(1);11–20.
24. F. Gonçalves, J.C. Gonçalves, A.C. Ferrão, P. Correia and R. Guiné. *Open Agriculture*, 2020;**5**(1);857–870.
25. Adegbaju, G.A. Otunola and A.J. Afolayan. Heliyon. 2020;2;6(6).
A. Roy and Bharadvaja. *Biomimetic and Nanobiomaterials*, 2018;**8**(2);1-9.

26. S.C.G. Daniel, L.A.N. Julius and S.S. Gorthi. *Sensors and Actuators B: Chemical*, 2017;**238**;641-650.
27. M. Kandiah and K.N. Chandrasekaran. *Hindawi Journal of Nanotechnology*, 2021;1-18.
28. B. Khanzada, N. Akthar, M.Z. Bhatti, H. Ismail, M. Alqarni, B. Mirza, G. Mostafa-Hedeab and G.E. Batiha. *Hindawi Journal of Chemistry*, 2021;1-16.
29. S.O. Aisida, K. Ugwu, P.A. Akpa, A.C. Nwanya, U. Nwankwo, S. Botha, P.M. Ejikeme, I. Ahmad, M. Maaza and F.I. Ezema. *Surfaces and Interfaces*, 2019;17.
30. L. Lin, L. Yi, L. Jiashen, L. Yao, A. Mak, F. Ko and Q. Ling. *Journal of Nanomaterials.* 2009;**4**;1–5.
31. S.T. Galatage, A.S. Hebalkar, S.V. Dhobale, O.R. Mali, P.S. Kumbhar, S.V. Nikade and S.G. Killedar. *CHAPTER METRICS OVERVIEW*, 2021;4.
32. M. Sweet and I. Singleton. Advances in *Applied Microbiology*, 2011;**77**;115-133.
33. R. Güzel and G. Erdal. *Silver Nanoparticles - Fabrication, Characterization and Applications. InTech*, 2017;**1**.
34. S. Iravani, H. Korbekandi, S.V. Mirmohammadi and B. Zolfaghari. *Research in pharmaceutical sciences*, 2-14;**9**(6);385-406.
35. S. Chandra and D.S. Rawat. *A review of ethno-medicinal uses and pharmacological properties*, 2015;**4**(3);123–131.
36. J.M Lü, P.H. Lin, Q. Yao and C. Chen. *Journal of Cellular and Molecular Medicine*, 2010;**14**(4);840-860.
37. D.A.A. Makuasa and P. Ningsih. *Journal of Applied Science, Engineering, Technology, and Education*, 2020;**2**(1);11-17.
38. F. Ahmed and M. Iqbal. *Organic & Medicinal Chemistry International Journal*, 2018;**5**(4).
39. X. Zhou, M. Wang, H. Li, S. Ye and W. Tang. *Frontiers in Nutrition*, 2023;10.
40. L. Shi, W. Zhao, Z. Yang, V. Subbiah and H.A.R. Suleria. *Science and Pollution Research*, 2022;**29**;81112-81129.
41. Y. Martono, F.F. Yanuarsih, N.R. Aminu and J. Muninggar. *Journal of Physics: Conference Series*, 2019;**1307**(1);012014.
42. J. Fowsiya and G. Madhumitha. IOP *Conference Series: Materials Science and Engineering*, 2019;**263**(2).
43. C. Wan, Y. Yu, S. Zhou, W. Liu, S. Tian and S. Cao. *Pharmacogn Mag*, 2011;**7**(25);40–40.
44. I.R.S. Bunghez, M. Barbinta, N. Badea, S.M. Doncea, A. Popescu and R.M. Ion. *Journal of Optoelectronics and Advanced Materials*, 2011;**14**(11);11-12.
45. H.P. Suresha. *Medium*, 2021.
46. D. Nettleton. *Commercial Data Mining*, 2014;79–104.
47. E.M. Njoya. *Cancer (Second Edition)*, 2021;349–357.
48. M. Ikram, A. Raza, M. Imran, A. Ul-Hamid, A. Shahbaz and S. Ali. *Nanoscale Research Letters*, 2020;**15**(95).
49. M.B. Sumi, A. Devadiga, V.S.K. and S.M.B. *Journal of Experimental Nanoscience*.
50. K. Sharma, S. Pandit, A.S. Mathuriya, P.K. Gupta, K. Pant and D.A. Jadhav. *Water*, 2023;**15**(1);56–56.
51. C. Xu. *Acta Physica Sinica -Chinese Edition*, 2012;**28**(5);1030-1036.
52. S.K. Kansal, M. Singh, and D. Sud. *Journal of Hazardous Materials*, 2007;**141**(3);581-9.
53. C.K. Githala, S. Raj, A. Dhaka, S.N. Mali and R. Trivedi. *Frontiers in Chemistry*, 2022;**10**;2296-2646.
54. S. Siddiquee, S. Saallah, N.A. Bohari, G. Ringgit, J. Roslan, L. Naher and N.F.H. Nudin. *Nanomaterials*, 2021;**11**(5);1142.
55. K. Ramalingam, T. Devasena, B. Senthil, R. Kalpana and R. Jayavel. *IET Science, Measurement & Technology*, 2017;**11**(2);171–178.
56. P. Allawadhi, V. Singh, A. Khurana, I. Khurana, S. Allwadhi, P. Kumar, A.K. Banothu, S. Thalugula, P.J. Barani, R.R. Naik and K.K. Bharani. *Sensors International*, 2021;**2**;2666-3511.
57. A. Roy, O. Bulut, S. Some, A.K. Mandal and M.D. Yilmaz. *RSC Advances*, 2019;**5**.
58. C.N. Banti and S.K. Hadjikakou. *Bio-protocol*, 2021;**11**(2).